Journal of Sol-Gel Science and Technology (2018) 85:506–513
https://doi.org/10.1007/s10971-017-4566-x

REVIEW PAPER: SOL-GEL AND HYBRID MATERIALS FOR ENERGY, ENVIRONMENT AND BUILDING APPLICATIONS

Preparation of tetraethoxysilane-based silica aerogels with polyimide cross-linking from 3, 3′, 4, 4′-biphenyltetracarboxylic dianhydride and 4, 4′-oxydianiline

Zhifang Fei[1,2] · Zichun Yang[1,2] · Guobing Chen[1,2] · Kunfeng Li[1,2]

Received: 9 September 2017 / Accepted: 14 December 2017 / Published online: 30 January 2018

Abstract

Polyimide cross-linked silica aerogels with different weight percentages of polyimide were prepared through sol–gel technology and supercritical CO_2 fluid drying technology. Tetraethoxysilane (TEOS) was used as a silica source precursor, 3-aminopropyltriethoxysilane (APTES) end-capped polyimide was used as a cross-linking agent, derived from 3, 3′, 4, 4′-biphenyltetracarboxylic dianhydride (BPDA) and 4, 4′-oxydianiline (ODA). The acid produced during the imidization process catalyzed the hydrolysis reaction without additional catalyst. After condensation reaction catalyzed by ammonium hydroxide solution, the polyimide cross-linked silica gels were obtained and then dried in supercritical CO_2. The polyimide cross-linked silica aerogels have low density (0.132~0.187 g/cm^3), high specific surface area (623–741 m^2/g), low thermal conductivity (0.0306~0.0347 W/m K at room temperature), relatively high compressive strength (1.03~3.82 MPa) and high thermal decomposition temperature (360 °C). This research provided a simple and efficient method that used the polyimide as a strengthening phase to improve the mechanical properties of TEOS-based silica aerogels.

Graphical abstract

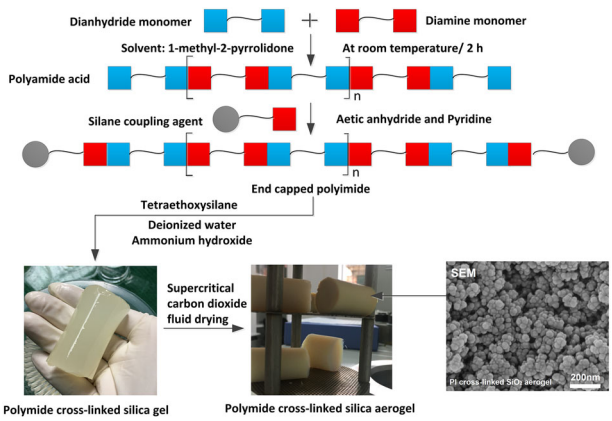

Keywords Silica aerogel · Polyimide · Thermal stability · Sol–gel preparation

✉ Zhifang Fei
fzf_js@126.com

[1] School of Power Engineering, Naval University of Engineering, 430033 Wuhan, Hubei, China

[2] Institute of High Temperature Structural Composite Materials of Naval Ship, Naval University of Engineering, 430033 Wuhan, Hubei, China

1 Introduction

Silica aerogels have continuous three-dimensional network structures composed of nanoscale pores and solid particles. This typical microstructure gives them extremely low density (0.003–0.35 g/cm^3), high porosity (80–99%), high specific surface area (500–1200 m^2/g), and extraordinarily

low thermal conductivity (0.013–0.04 W/m K). Silica aerogels have tremendous application value in the field of aerospace, building, marine and so on [1–5]. However, they are usually flimsy and fragile due to the weak bonding force between solid phase particles, which hinder their large-scale engineering applications [6]. To date, the methods of mechanical enhancement of silica aerogels with fibers, such as ceramic fibers [7–9], glass fibers [10, 11], carbon fibers [12], have been relatively mature. However, the density of the fiber-reinforced silica aerogel composite materials increase significantly, so that their thermal insulation performances reduce consequently. What makes it worse, powder or the granule form of this type of composite aerogels caused by the poor interface combination between the fibers and the aerogels greatly restrains their engineering application.

In recent years, improving the mechanical properties of silica aerogels by the method of cross-linking with a polymer has become a hot research topic. The polymer cross-linked silica aerogel can keep the unique three-dimensional network nano-structures, and the density of this material will not significantly increase. These advantages are helpful for maintaining the super thermal insulation property. Usually the silica gels are soaked in a monomer bath and cross-linked by oligomers. And then a polymer layer is formed on the surface of silica primary particles with chemical bonds combination which can enhance the interface bonding strength between the particles [13] and effectively improves the mechanical properties of the silica aerogels. It has been reported that some different oligomers such as isocyanate [14–16], epoxy [17–22] styrene [23–25], and cyanoacrylates [26–29] can be used to reinforce the silica aerogel. However, the decomposition temperature of these polymers are below 400 °C, which limits the scope of application.

Polyimides (PIs) have excellent thermal stability, thermal oxidation resistance, and mechanical properties [30]. Until now, although a lot of researches for polymer cross-linked silica aerogels were reported in literature, there was a lack of the preparation methods of silica aerogels reinforced with PIs. In several previous reports, tetramethoxysilane (TMOS) [31] and methyltrimethoxysilane (MTMS) [32] were used as silicon source precursors. As we all know, comparing to TMOS tetraethoxysilane (TEOS) has lower toxicity. Besides, TEOS-based silica aerogels usually have higher thermal stability than MTMS-based aerogels. This is because that the oxidation of methyl ($-CH_3$) group present in the MTMS lead to the decrease of thermal stability.

In this study, a relatively simple method was proposed to prepare TEOS-based silica aerogels reinforced with PIs. As shown in Fig. 1, APTES was used to produce a end-capped polyamide acid (PAA) by reacting with terminal anhydride groups of oligomers derived from 3, 3′, 4, 4′-biphenyltetracarboxylic dianhydride (BPDA). The three-dimensional hybrid silica networks were created by the reaction between TEOS and water in alkaline conditions, followed by the condensation polymerization with the APTES end-capped PI which had completed the chemical imidization process. The significant advantage of the method is that the hydrolysis reaction of the silicon source precursor was catalyzed by the acid produced during the imidization process without adding additional acid catalyst. And compared with the method of soaking gels in solution, this method has other advantages such as great efficiency, easy accessibility, and

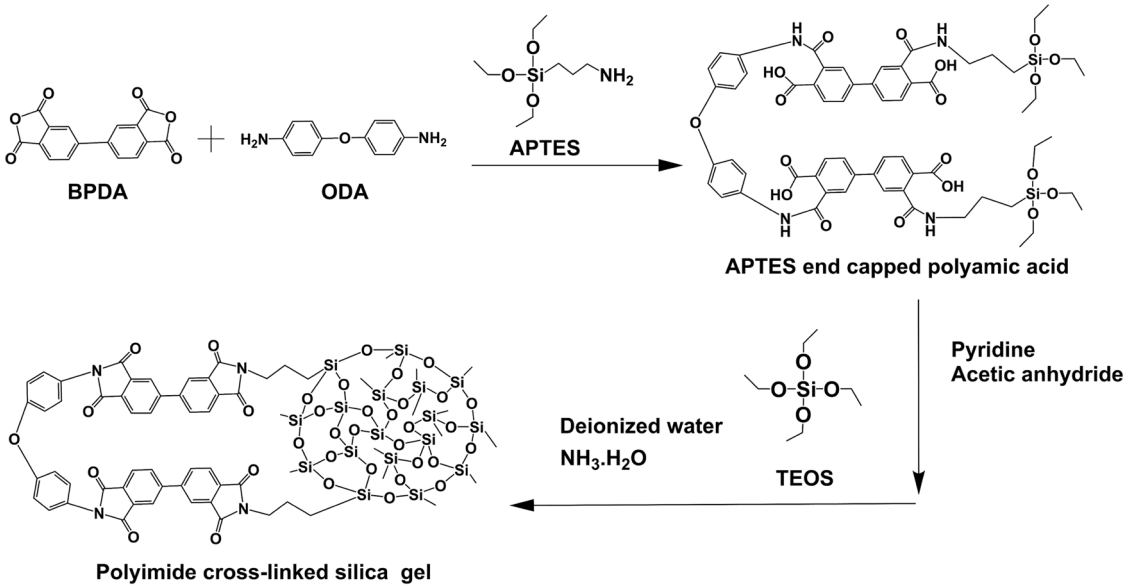

Fig. 1 Synthesis of the PI cross-linked SiO_2 hybrid gel

short preparation period. In addition to above, the influence of different mass percentages of PIs on the microstructure, mechanical and thermal properties of PI cross-linked silica aerogels was also studied.

2 Materials and methods

2.1 Materials

Tetraethoxysilane (TEOS, AR), 3, 3′, 4, 4′-biphenyltetracarboxylic dianhydride (BPDA, AR), 4, 4′-oxydianiline (ODA, AR), 3-aminopropyltriethoxysilane (APTES, AR), 1-methyl-2-pyrrolidone (NMP, AR), pyridine (AR), ammonium hydroxide solution (28.0~30.0%, NH_3 basis), hydrochloric acid (HCL, AR), and ethanol (EtOH, AR) were purchased from Aladdin Industrial Corporation, China. Acetic anhydride (AR) was purchased from Sinopharm Chemical Reagent Cor. Ltd, China.

2.2 The preparation of PI cross-linked SiO_2 aerogels

TEOS (13.55 ml) and deionized water (3.78 ml) were mixed with NMP (40 ml) to form Solution A. Then, BPDA (0.719 g) was slowly added to the solution of ODA (0.242 g) in 30 ml NMP. The mixed solution was stirred for 2 h at room temperature. Then APTES (0.575 ml) was added and end capped with PAA oligomers for 1 h. The molar ratio of BPDA: ODA: APTES was 1:2.02:2.02. The acetic anhydride (1.867 ml) and pyridine (1.594 ml) were added and stirred to carry out the chemical imidization process to form Solution B. After mixing Solution A with Solution B, the hydrolysis process was catalyzed by the acid produced by chemical imidization process and stirring at 50 °C for 3 h. After hydrolysis, a mixture of ammonium hydroxide and NMP was slowly added until the pH value reach about 7.5. The mixture solution was continually stirred for 10 min, then was poured into a polytetrafluoroethylene mold. The PI cross-linked SiO_2 gels were obtained after gelation at 40 °C within 20 min. After aging for 24 h, the gels were removed from the mold, and the solvent within the wet gels was exchanged with EtOH three times (for 8 h each time). Then the wet gels were placed in a supercritical fluid extraction chamber filled with EtOH, and exchanged with supercritical CO_2 at 10 MPa and 50 °C for 48 h. Lastly, the PI cross-linked SiO_2 aerogels were obtained after gaseous CO_2 was slowly exhausted out from the chamber over 8 h. The native SiO_2 aerogels were prepared by the two step sol–gel method with hydrochloric acid and ammonium hydroxide acting catalyzers. First, the mixture of TEOS, acid water and NMP was stirred for 3 h at 50 °C to complete the hydrolysis process. Second, a mixture of ammonium hydroxide and NMP was slowly added and then silica gels were obtained within 15 min. The molar ratio of TEOS:H_2O:HCL:NH_4OH:NMP was $1{:}3.5{:}3.6 \times 10^{-3}{:}2.8 \times 10^{-3}{:}10$. The chemical composition of PI cross-linked SiO_2 aerogels with different mass fraction of PI and the native SiO_2 aerogels is presented in Table 1.

2.3 Characterization

The specific surface area and pore size distribution were obtained from nitrogen adsorption–desorption isotherms using a surface analyzer (ASAP 2020, Micromeritics Instrument Corp, USA) at 77 K. The microstructure of the aerogels was observed by a scanning electron microscope (Hitachi SU8010, Hitachi High Technologies Corp, Japan). The mechanical properties of some cylindrical samples with size of about 18 mm in diameter and 30 mm in length were measured by a compression test with an Electronmechanical Universal Testing System (MTS Criterion Model 45, MTS

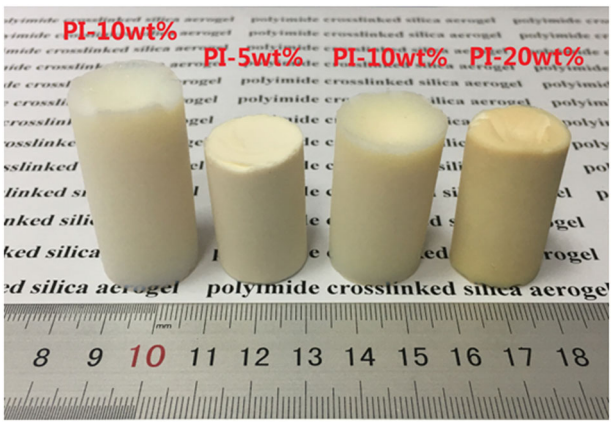

Fig. 2 The PI cross-linked SiO_2 aerogels with different weight percentages of PI

Table 1 The chemical composition of the PI cross-linked SiO_2 aerogel with different mass fraction of PI

Sample	PI (wt%)	TEOS (ml)	H_2O (ml)	ODA (g)	BPDA (g)	APTES (ml)	Pyridine (ml)	Acetic anhydride (ml)
Native SiO_2 aerogel	0	13.55	3.78	0	0	0	0	0
PI-5wt%	5	13.55	3.78	0.049	0.147	0.118	0.325	0.381
PI-10wt%	10	13.55	3.78	0.104	0.309	0.247	0.685	0.802
PI-20wt%	20	13.55	3.78	0.242	0.719	0.575	1.594	1.867

Table 2 The detailed properties of the PI cross-linked SiO_2 aerogel

Sample	Density (g/cm^3)	Shrinkage (%)	Specific surface area (m^2/g)	Pore volume (cm^3/g)	Average pore diameter (nm)
PI-5wt%	0.132	15.8	741	2.54	13.69
PI-10wt%	0.153	18.6	693	2.38	13.70
PI-20wt%	0.187	25.5	623	2.25	14.41

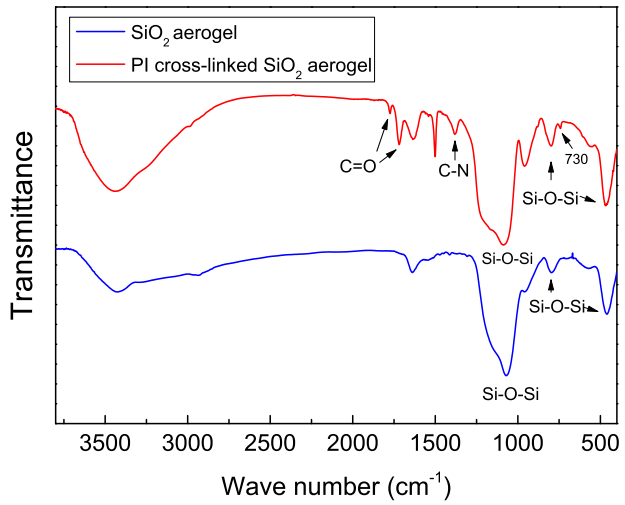

Fig. 3 FTIR spectrum of the native SiO_2 aerogel and the PI cross-linked SiO_2 aerogel

System Corp, USA) with a constant loading speed at 1.5 mm/min. Thermal conductivity was measured by a thermal constant analyzer (TPS 2500 S, Hot Disk AB, Sweden) at room temperature. The chemical structure of the aerogels was confirmed by Fourier transform infrared spectroscopy (NICOLET 5700 FTIR Spectrometer, Thermo Nicolet Corp, USA). The thermal stability test was performed in air by Thermo gravimetric analysis from room temperature to 800 °C (TG/DTA6300, Seiko Instruments Inc, Japan).

3 Results and discussion

PI cross-linked silica aerogels with different weight percentages of PI are shown in Fig. 2. The samples keep the shape well as before drying and have a smooth surface and no cracks. The samples won't drop the powder when they are touched. From Table 2 it can be obtained, with PI mass fraction increasing from 5 to 20%, the density of the samples increases from 0.132 to 0.187 g/cm^3 and the radial shrinkage rate increased from 15.8 to 25.5%.

Figure 3 shows the FTIR spectra of the native SiO_2 aerogel and PI cross-linked SiO_2 aerogel. Peaks at 1087, 795 and 464 cm^{-1} all represent Si–O–Si bond of silica. The FTIR spectrum of PI cross-linked SiO_2 aerogel has distinctive peaks from imide C=O at 1776 cm^{-1}, 1720 cm^{-1} and stretching vibration absorption of C–N at 1380 cm^{-1}. The peak of 730 cm^{-1} represents the bending vibration absorption of the imide ring.

Figure 4 shows the SEM micrographs of aerogel samples with different weight percentages of PI. As we can see, PI cross-linked SiO_2 aerogels have uniform three-dimensional network structures composed of the spherical particles with particle diameters in the range of 20–50 nm similar to those of native SiO_2 aerogels. This typical microstructure can inhibit the heat transfer inside the material and contribute to improve the insulation performance of the samples. In contrast, from Fig. 4b–d, we can see that the contact areas between the particles of PI cross-linked SiO_2 aerogels is larger than those of native SiO_2 aerogels. On the one hand, this is because that silica particals have been combined with the PI via covalent bonds. One the other hand, it is also due to the larger shrinkage caused by PI during drying. So, the PI chains can reinforce the weak bonding strength between silica particles and reduce the powder, which is beneficial for the improvement of the mechanical properties of the aerogels.

The specific surface area and pore volume of the PI cross-linked SiO_2 aerogels were measured by nitrogen sorption using the Branuaer-Emmet-Teller method. The specific surface area of as-prepared PI cross-linked SiO_2 aerogel monoliths are in the range of 623~741 m^2/g, which is larger than those previous reported (463.2~582.7 m^2/g) [32]. The larger specific surface area can increase the gas-solid heat transfer resistance on the surface of the hole structure, reduce the heat transfer, and then improve the insulation performance of materials. Figure 5 shows the typical nitrogen adsorption–desorption isotherms of the PI cross-linked SiO_2 aerogels. As we can see, the adsorption isotherms rise slowly at low relative pressure ($P/P_0 < 0.8$) and rise significantly at high relative pressure ($P/P_0 > 0.8$). According to the classification of adsorption isotherms proposed by International Union of Pure and Applied Chemistry (IUPAC), the adsorption isotherms are type IV curves with H_1 hysteresis loop. This type of absorption curve shows that the material has uniformly distributed spherical particle clusters and cylindrical mesopores (2~50 nm) [33]. As we can see from Fig. 6, the pore size distribution peaks at about 30 nm but trails out to about 100 nm. The average pore sizes and pore volume of PI cross-linked SiO_2 aerogels are listed in Table 2.

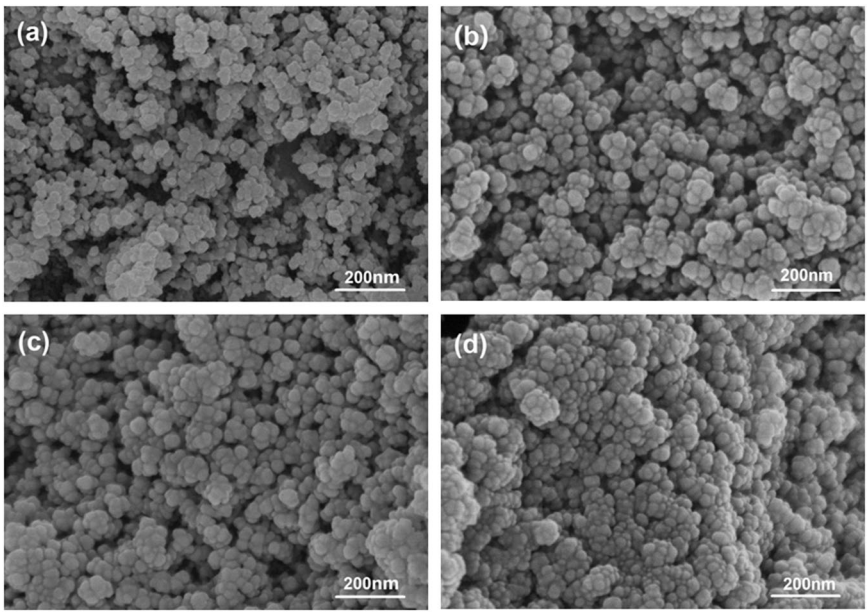

Fig. 4 SEM micrographs of aerogel samples with different weight percentages of PI: **a** 0 wt%; **b** 5 wt%; **c** 10 wt%; **d** 20 wt%

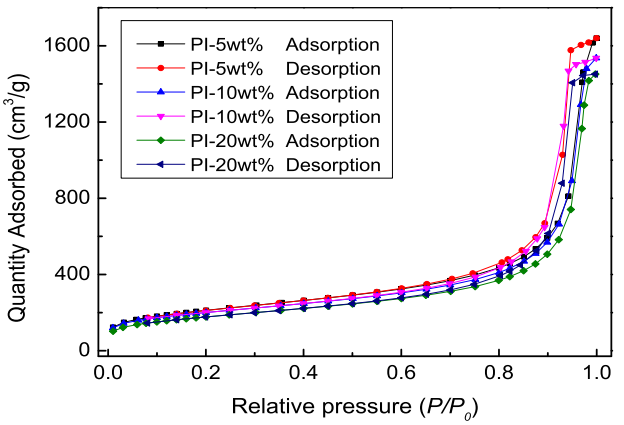

Fig. 5 N_2 adsorption–desorption isotherms of the PI cross-linked SiO_2 aerogels

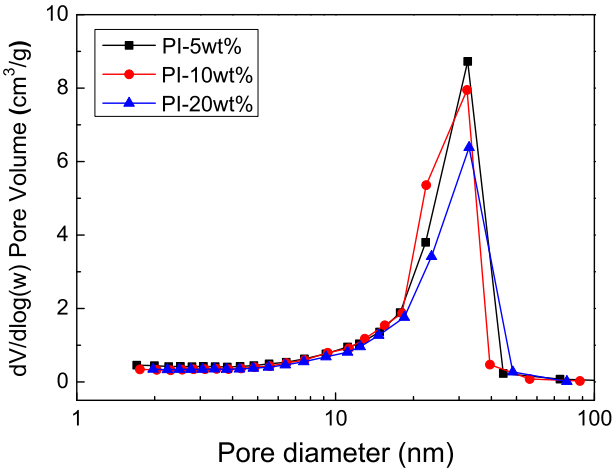

Fig. 6 Pore size distributions of the PI cross-linked SiO_2 aerogels

Three large-scale samples at each PI content were prepared and thermal conductivity values of these samples including native silica aerogels were measured three times at room temperature. Then the average values were calculated. As we can see from the Fig. 7, the average thermal conductivity of the PI cross-linked aerogels is 0.0306~0.0347 W/m K, which is slightly higher than that of the native silica aerogel (0.0296 W/m K). The low thermal conductivity has close relationship with their unique three-dimensional network nanostructures. On the one hand, the nanoscale skeleton of the aerogel greatly extends the heat conduction path and increases the thermal resistance. On the other hand, the gas convection heat transfer in the pore is sufficiently suppressed because the pore size is mainly smaller than the mean free path of free air (70 nm). As a result, the PI cross-linked aerogel exhibits superior thermal

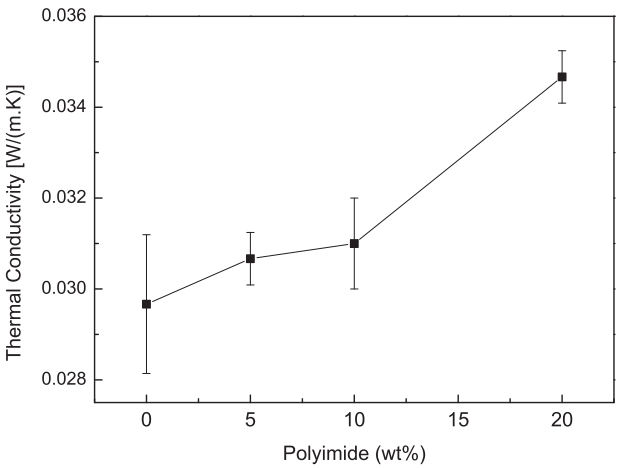

Fig. 7 Thermal conductivity of the aerogel samples

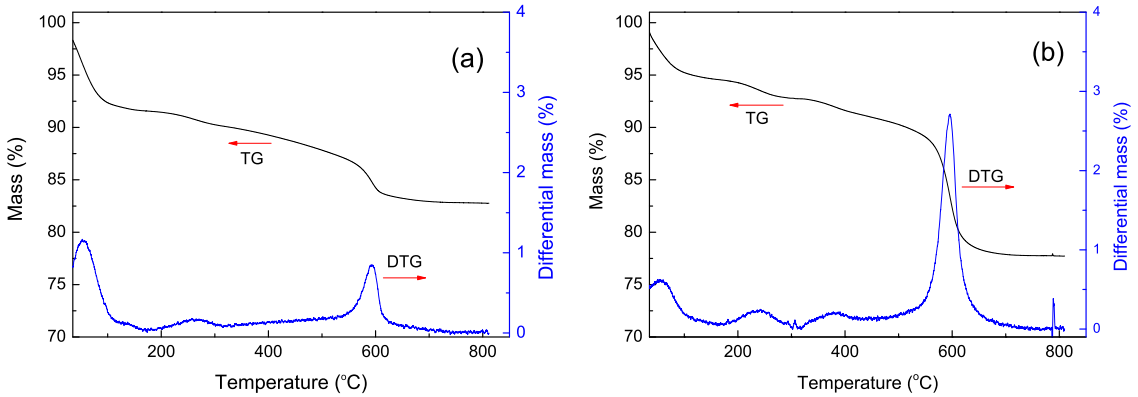

Fig. 8 TGA curves of the PI cross-linked SiO_2 aerogels, (**a**) PI-5wt%, (**b**) PI-10wt%

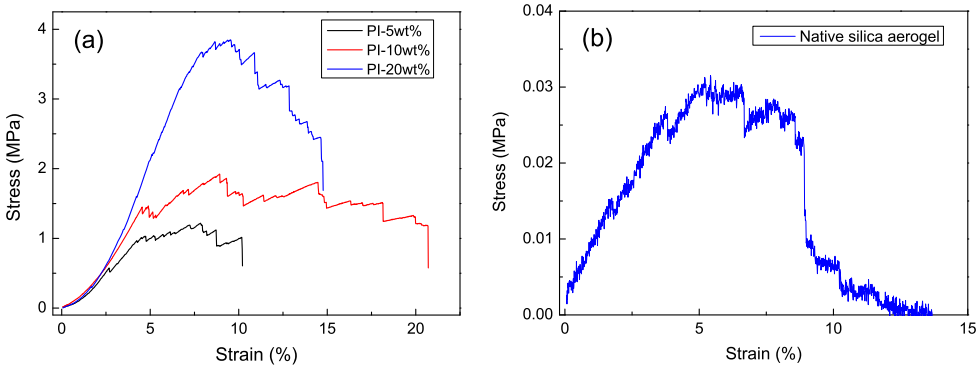

Fig. 9 Compressive stress–strain curves of the samples, (**a**) PI cross-linked SiO_2 aerogel, (**b**) native SiO_2 aerogel

Table 3 Mechanical properties of PI cross-linked SiO_2 aerogels

Samples	Compressive strength (MPa)	Young's modulus (MPa)
Native SiO_2 aerogel	0.027	0.71
PI-5wt%	1.03	21.70
PI-10wt%	1.44	30.14
PI-20wt%	3.82	44.16

insulation performance to the other traditional macroporous insulation materials. We can see that the thermal conductivity increases with the increase of the PI contents. This is because the increase of the PI content causes the increase of the particle size and contact area between the particles. What's more, the network structures of the aerogels are more compact, which leads to the increase of the solid heat conduction.

As is shown in Fig. 8, the thermal gravimetric analysis of the PI cross-linked SiO_2 aerogels (PI-5 and PI-10 wt%) was tested in air from room temperature to 800 °C. The weight loss is less than 7% from room temperature to 100 °C, which corresponds to the absorption of water and ethanol. The weight loss starting at 200 °C is due to the evaporation of a small amount of NMP and water produced of heat imidization process. The weight loss with the onset of 360 °C is caused by degradation of propyl groups from APTES. The large mass loss from around 500 °C is because of the decomposition of PI [31]. So, the decomposition temperature of PI cross-linked SiO_2 aerogels should be around 360 °C, which is similar to that of the clay reinforced PI/silica hybrid aerogel [31]. It is higher than that of polyurea (200 °C) [16] and polyacrylate (230 °C) [28] cross-linked aerogels, but similar to that of epoxy (370 °C) [20] and polystyrene (380 °C) [23] cross-linked aerogels. In addition, the mass loss from 300 to 500 °C of PI cross-linked SiO_2 aerogels is much less than that of other polymer cross-linked SiO_2 aerogels. It is because that PIs have not begun to decompose in this temperature range.

The typical stress-strain curves of the PI cross-linked SiO_2 aerogel samples with different PI contents and the native SiO_2 aerogel are shown in Fig. 9. The compression strength and Young's modulus of the samples are listed in Table 3. We can see that, the compression strength and Young's modulus increase with the increase of PI contents. When the weight percentage of PI is up to 20%, the compression strength and Young's modulus of the PI cross-linked SiO_2 aerogel is about 140 times larger than those of native SiO_2 aerogel. Therefore, the cross-linked aerogels in this work

show good mechanical properties. As we can see from stress–strain curves of PI cross-linked SiO_2 aerogels in Fig. 9, when the stress reaches the maximum value, brittleness crack doesn't occur directly and violently. This is because that the silica skeleton strengthened by the resilient PI chains.

4 Conclusions

The PI cross-linked SiO_2 aerogel monoliths with nanoscale three-dimensional network structures were prepared by the method of sol–gel technology and supercritical fluid drying technology. PI chains were successfully combined with silica primary particles through cross-linking reaction. The introduction of the PI increased the binding strength between silica nanoparticles, and the mechanical properties of silica aerogels were improved significantly. The maximum values of the compressive strength (3.82 MPa) and the Young's modulus (44.16 MPa) are respectively around 140 times of the native silica aerogel. The PI cross-linked SiO_2 aerogel exhibits excellent thermal insulation and thermal stability with low thermal conductivity (0.0306~0.0347 W/m K at room temperature), and relatively high decomposition temperature (360 °C). Therefore, this material has great application potential in the fields of ship, aircraft, building and so on.

Acknowledgements This work was supported by the National Natural Science Foundation of China (Grant No. 51702364) and Independent Project of Naval University of Engineering, China (Grant No. 425517K152).

Compliance with ethical standards

Conflict of interest The authors declare that they have no conflict of interest.

References

1. Hrubesh LW (1998) Aerogel applications. J Non-Cryst Solids 225:335–342
2. Morris CA, Anderson ML, Stroud RM, Merzbacher CI, Rolison DR (1999) Silica sol as a nanoglue: flexible synthesis of composite aerogels. Science 284:622–624
3. Pierre AC, Pajonk GM (2002) Chemistry of aerogels and their applications. Chem Rev 102:4243–4266
4. Koebel M, Rigacci A, Achard P (2012) Aerogel-based thermal superinsulation: an overview. J Sol-Gel Sci Technol 63:315–339
5. Cuce E, Cuce PM, Wood CJ, Riffat SB (2014) Toward aerogel based thermal superinsulation in buildings: a comprehensive review. Renew Sustain Energy Rev 34:273–299
6. Aegerter MA, Leventis N, Koebel MM (2011) Aerogels handbook. Springer-Verlag, New York, NY
7. Karout A, Buisson P, Perrard A, Pierre AC (2005) Shaping and mechanical reinforcement of silica aerogel biocatalysts with ceramic fiber felts. J Sol-Gel Sci Technol 36:163–171
8. Yang J, Li S, Luo Y, Wang F (2011) Compressive properties and fracture behavior of ceramic fiber-reinforced carbon aerogel under quasi-static and dynamic loading. Carbon 49:1542–1549
9. Gao QF, Feng J, Zhang CR, Feng JZ, Wu W, Jiang YG (2009) Mechanical properties of ceramic fiber-reinforced silica aerogel insulation composites. J Chin Ceram Soc 37:1–5
10. Yuan B, Ding S, Wang D, Wang G, Li H (2012) Heat insulation properties of silica aerogel/glass fiber composites fabricated by press forming. Mater Lett 75:204–206
11. Liao YD, Wu HJ, Ding YF (2012) Engineering thermal and mechanical properties of flexible fiber-reinforced aerogel composites. J Sol-Gel Sci Technol 63:445–456
12. Meador MAB, Vivod SL, Mccorkle L, Quade D, Sullivan RM, Ghosn LD, Clark N, Capadona LA (2008) Reinforcing polymer cross-linked aerogels with carbon nanofibers. J Mater Chem 18:1843–1852
13. Zhang G, Dass A, Rawashdeh AMM, Thomas J, Counsil JA, Leventis CS, Fabrizio EF, Ilhan F, Vassilaras P, Scheiman DA, Mccorkel L, Palczer A, Johnston CJ, Meador MA, Leventis N (2004) Isocyanate-cross-linked silica aerogel monoliths: preparation and characterization. J Non-Cryst Solids 350:152–164
14. Capadona LA, Meador MAB, Alunni A, Fabrizio E, Vassilaras P, Leventis N (2006) Flexible, low-density polymer cross-linked silica aerogels. Polymer 47:5754–5761
15. Sabri F, Marchetta J, Smith KM (2013) Thermal conductivity studies of a polyurea cross-linked silica aerogel-RTV 655 compound for cryogenic propellant tank applications in space. Acta Astronaut 91:173–179
16. Yang H, Kong X, Zhang Y, Wu C, Cao E (2011) Mechanical properties of polymer-modified silica aerogels dried under ambient pressure. J Non-Cryst Solids 357:3447–3453
17. Meador MAB, Fabrizio EF, Ilhan F, Dass A, Zhang G, Vassilaras P, Johnston JC, Leventis N (2005) Cross-linking amine-modified silica aerogels with epoxies: mechanically strong lightweight porous materials. Chem Mater 17:1085–1098
18. Meador MAB, Scherzer CM, Vivod SL, Quade D, Nguyen BN (2010) Epoxy reinforced aerogels made using a streamlined process. ACS Appl Mater Interfaces 2:2162–2168
19. Ge D, Yang L, Li Y, Zhao JP (2009) Hydrophobic and thermal insulation properties of silica aerogel/epoxy composite. J Non-Cryst Solids 355:2610–2615
20. Ahmad Z, Al-Sagheer F (2015) Novel epoxy-silica nano-composites using epoxy-modified silica hyper-branched structure. Progress Org Coat 80:65–70
21. Shao Z, Wu G, Cheng X, Zhao Y (2012) Rapid synthesis of amine cross-linked epoxy and methyl co-modified silica aerogels by ambient pressure drying. J Non-Cryst Solids 358:2612–2615
22. Randall JP, Meador MAB, Jana SC (2013) Polymer reinforced silica aerogels: effects of dimethyldiethoxysilane and bis (trimethoxysilylpropyl) amine as silane precursors. J Mater Chem A 1:6642–6652
23. Mirshafiei-Langari SA, Haddadi-Asl V, Roghani-Mamaqani H, Sobani M, Khezri K (2013) Synthesis of hybrid free and nanoporous silica aerogel-anchored polystyrene chains via in situ atom transfer radical polymerization. Polym Compos 34:1648–1654
24. Mirshafiei-Langari SA, Roghani-Mamaqani H, Sobani M, Sobani M, Khezri K (2013) In situ atom transfer radical polymerization of styrene in the presence of nanoporous silica aerogel: kinetic study and investigation of thermal properties. J Polym Res 20:163
25. Maleki H, Durães L, Portugal A (2015) Synthesis of mechanically reinforced silica aerogels via surface-initiated reversible addition-fragmentation chain transfer (RAFT) polymerization. J Mater Chem A 3:1594–1600
26. Mulik S, Sotiriou-Leventis C, Churu G, Lu H, Leventis N (2008) Cross-linking 3D assemblies of nanoparticles into mechanically

strong aerogels by surface-initiated free-radical polymerization. Chem Mater 20:5035–5046
27. Maleki H, Durães L, Portugal A (2014) Synthesis of lightweight polymer-reinforced silica aerogels with improved mechanical and thermal insulation properties for space applications. Microporous Mesoporous Mater 197:116–129
28. White LS, Bertino MF, Saeed S, Saoud K (2015) Influence of silica derivatizer and monomer functionality and concentration on the mechanical properties of rapid synthesis cross-linked aerogels. Microporous Mesoporous Mater 217:244–252
29. White LS, Bertino MF, Kitchen G, Young J, Newton C, Alsoubaihi R, Saeed S, Saoud K (2015) Shortened aerogel fabrication times using an ethanol–water azeotrope as a gelation and drying solvent. J Mater Chem A 3(2):762–772
30. Matsuura T, Yamada N, Nishi S, Hasuda Y (1993) Polyimides derived from 2,2′-bis (trifluoromethyl)-4, 4′-diaminobiphenyl. III: properties control for polymer blends and copolymerization of fluorinated polyimides. Macromolecules 26:419–423
31. Guo J, Nguyen BN, Li L, Meador MAB, Scheiman DA, Cakmak M (2013) Clay reinforced polyimide/silica hybrid aerogel. J Mater Chem A 1(24):7211–7221
32. Yan P, Zhou B, Du A (2014) Synthesis of polyimide cross-linked silica aerogels with good acoustic performance. RSC Adv 4:58252–58259
33. Rao AP, Pajonk GM, Rao AV (2005) Effect of preparation conditions on the physical and hydrophobic properties of two step processed ambient pressure dried silica aerogels. J Mater Sci 40:3481–3489